Observing the multiverse with cosmic wakes

Matthew Kleban, Thomas S. Levi, and Kris Sigurdson

Phys. Rev. D **87**, 041301 — Published 21 February 2013

DOI: 10.1103/PhysRevD.87.041301

Observing the Multiverse with Cosmic Wakes

Matthew Kleban,[1,*] Thomas S. Levi,[2,†] and Kris Sigurdson[2,‡]

[1] *CCPP, Department of Physics, New York University, New York, NY 10003, USA*
[2] *Department of Physics and Astronomy, University of British Columbia, Vancouver, BC V6T 1Z1, Canada*

Current theories of the origin of the Universe, including string theory, predict the existence of a multiverse with many bubble universes. These bubble universes may collide, and collisions with ours produce *cosmic wakes* that enter our Hubble volume, appear as unusually symmetric disks in the cosmic microwave background (CMB) and disturb large scale structure (LSS). There is preliminary evidence consistent with one or more of these disturbances on our sky. However, other sources can produce similar features in the CMB and so additional signals are needed to verify their extra-universal origin. Here we find, for the first time, the detailed 3D shape, temperature and polarization signals of the cosmic wake of a bubble collision consistent with current observations. The polarization pattern has distinct features that when correlated with the corresponding temperature pattern are a unique and striking signal of a bubble collision. These features represent a verifiable prediction of the multiverse paradigm and might be detected by current or future experiments. A detection of a bubble collision would confirm the existence of the Multiverse, provide compelling evidence for the string theory landscape, and sharpen our picture of the Universe and its origins.

Introduction: The possibility of observing cosmic bubble collisions has received considerable attention (see, e.g., [1, 2] for recent reviews). Such collisions are predicted by multiple-vacua models like the string theory landscape, and observing one would fundamentally alter our understanding of the cosmos. In these models the observed Universe is contained within a bubble formed in a first-order phase transition from a parent false vacuum. Collisions with other bubbles produces a special wave, a *cosmic wake*, that propagates into our bubble and affects the spacetime region to the causal future of the collision.

To a remarkable extent these events can be analyzed in a model-independent fashion. In this work we find the pattern of temperature and polarization of CMB photons induced by a cosmic wake using the cosmological Einstein-Boltzmann equations. The results are striking. Collisions may produce a unique polarization signal, a "double peak" in the polarization magnitude as a function of angle. This feature, and more generally a large-scale circularly symmetric polarization and temperature pattern, serve as a true smoking gun for their detection. Moreover, this vital corroborating signal in polarization may be as easy to detect as the temperature signal. Our results also specify three-dimensional density and velocity perturbations after decoupling, which enables future work on the effect of the cosmic wake on LSS.

Background: The detailed effects of bubble collisions depend on unknown high-energy microphysics. Nevertheless, the physics of the cosmic wake that affects observables like the CMB and LSS depends only on a few parameters. This is because a collision between two bubbles is a highly symmetric event, and inflation in our Universe after the collision efficiently erases all but a few leading effects. For a broad class of models, four parameters are relevant to the observable Universe after inflation. One probes microphysics, while the others reflect initial conditions (the position and time the colliding bubble nucleated). These parameters specify the direction, distance, and strength of the cosmic wake we see, and thus the location, size, and intensity of the affected disc in the CMB sky.

As the primordial plasma supports acoustic waves, cosmic wakes can propagate in our Hubble volume. The most dramatic effect is two sharp peaks in E-mode polarization as a function of angle: two concentric rings of polarized light that line the affected CMB disc. These peaks are a position-space version of the acoustic peaks observed in the angular power spectrum of the CMB.

Scalar Perturbations: We first determine the scalar perturbations from a bubble collision that remain after a period of inflation and later form the cosmic wake.

The field-configuration describing the collision of two Coleman-de Luccia thin-wall bubbles preserves an $SO(2,1)$ group of isometries [3–6]. In suitable coordinates the collision occurs at one instant everywhere along a spacelike hyperbolic surface $\mathbb{H}_2$, and influences the spacetime to the future of that event. During inflation, up to slow-roll corrections, the metric is de Sitter space with Hubble constant H_I:

$$ds^2 = -(1+H_I^2t^2)^{-1}dt^2 + (1+H_I^2t^2)dx^2 + t^2 d\mathbb{H}_2^2,$$

with $d\mathbb{H}_2^2 = dr^2 + \sinh^2 r d\varphi^2$. The effects of the collision are uniform on the $\mathbb{H}_2$.

After N e-folds of inflation $H_I t \propto e^N$ is exponentially large and curvature is small. Current constraints show the curvature radius $R_0 \gtrsim 10c/H_0$, or $\sqrt{\Omega_k} = (R_0 H_0/c)^{-1} \lesssim 0.1$. We henceforth approximate curvature as small and treat the surface $\mathbb{H}_2$ as planar. Curvature and slow-roll effects induce small corrections. Finally, we use the thin-wall approximation. Finite wall thickness can alter small scale features in the signal.

* mk161@nyu.edu
† tslevi@phas.ubc.ca
‡ krs@phas.ubc.ca

The extent to which this happens is a model-dependent question and, interestingly, could provide further details about the microphysics. Specifically, if a distinct double peak is observed it demonstrates that the Hubble scale of the parent false vacuum H_F satisfies $H_F W H_F(2r_c + W) \lesssim 10^{-2}$, where $W < 1/H_f$ is the wall thickness, and $r_c < 1/H_f$ is the radius of the bubble when it formed [7]. If this bound is not satisfied, the polarization (and temperature) signal will be altered in a way that reflects the internal structure of the collision bubble's domain wall, an exciting prospect that deserves further study [7].

Including linear perturbations in conformal Newtonian gauge, the metric is

$$ds^2 = (H_I\tau)^{-2}\left[-(1+2\Phi)\,d\tau^2 + (1-2\Psi)\,d\vec{x}^2\right],$$

where τ is the conformal time, coordinates are chosen with the solar system's comoving location at $\vec{x}=0$, and Φ and Ψ are the Newtonian potentials. The spacetime region affected by the collision satisfies $x > -\tau + x_c$ for a constant x_c that depends on when the collision occurred. We focus on collisions with causal influence intersecting last scattering as these have the best prospect for detection [8–10]. As the Earth is at $x=0$ and $H_I|\tau| \ll 1$ after inflation $H_I|x_c| \ll 1$.

If inflation occured, pre-inflation inhomogeneities became perturbative early on, and thereafter obeyed linear cosmological perturbation theory [11]. At leading order, perturbations to the inflaton $\phi = \phi_0 + \delta\phi$ obey the equation of motion of a free scalar in de Sitter space,

$$\partial_\tau^2\delta\phi + 2\mathcal{H}\partial_\tau\delta\phi - \nabla^2\delta\phi + \mathcal{O}(\epsilon,\eta) = 0,$$

where $\mathcal{H}(\tau) = -1/\tau + \mathcal{O}(\epsilon,\eta)$ is the conformal Hubble constant, and ϵ,η are standard slow-roll parameters. When a perturbation is constant on planar surfaces the general solution can be written [8],

$$\delta\phi(\tau,x) = \tilde{g}(\tau+x) - \tau\tilde{g}'(\tau+x) + \tilde{f}(\tau-x) - \tau\tilde{f}'(\tau-x), \quad (1)$$

where $\tilde{f}$ and $\tilde{g}$ are arbitrary one-dimensional functions (and $\tilde{f}'$ and $\tilde{g}'$ their derivatives). To proceed we need the initial perturbation $\delta\phi$ from a bubble collision event. Consider the edge of the collision lightcone $x = -\tau_i + x_c$ at time $\tau_i \sim -H_I^{-1}$ near the start of inflation. As $\delta\phi$ is non-zero only for $x > -\tau_i + x_c$, we have

$$\tilde{g}(\tau + x - x_c) = g(\tau + x - x_c)\Theta(\tau + x - x_c)$$

and

$$\tilde{f}(\tau - x) = f(-\tau + x - x_c + 2\tau_i)\Theta(-\tau + x - x_c + 2\tau_i),$$

where Θ is a Heaviside step function. By the end of inflation $H_I|\tau_e| \ll 1$ and the terms proportional to f is non-zero only for $x - x_c > -2\tau_i \sim 2H_I^{-1}$. As we are only interested in $|x - x_c| \ll H_I^{-1}$ they are not relevant for cosmological observables.

At inflation-end, $\delta\phi$ is generically [7]

$$\begin{aligned}\delta\phi(\tau_e, x) &\approx g(x - x_c)\Theta(x - x_c) \\ &= M\sum_{n=0}^{\infty}\left\{\alpha_n H_I^n\,(x - x_c)^n\right\}\Theta(x - x_c).\end{aligned} \quad (2)$$

We drop terms proportional to $\tau_e \ll H_I^{-1}$, and expand g in a series with coefficients α_n. Model-dependent initial conditions $\delta\phi(\tau_i,x)$ and $\delta\dot{\phi}(\tau_i,x)$ determine α_n. Regular $\delta\phi$ have $\alpha_0 = 0$. For $\mathcal{O}(1)$ perturbation at early times $\tau_i \sim H_I^{-1}$ and generically $\alpha_n \lesssim 1$ for $n > 0$. As we are interested in $H_I|x - x_c| \ll 1$, higher order terms are negligible without fine-tuning. At inflation-end, the leading term is

$$\delta\phi = M\alpha_1(x - x_c)\Theta(x - x_c)\,. \quad (3)$$

This has two parameters ($M\alpha_1$ and x_c), and two angles specify the direction towards collision-center. These four parameters fully characterize observable effects of a generic collision.

Curvature Perturbations: The inflaton perturbation $\delta\phi$ sources a metric perturbation

$$\Phi = -\frac{V'}{2}g(\tau + \tilde{x})\Theta(\tau + \tilde{x}) \approx -\frac{V'}{2}M\alpha_1\tilde{x}\Theta(\tilde{x}),$$

where $\tilde{x} \equiv x - x_c$, $V' = \partial V(\phi)/\partial\phi$, and $V(\phi)$ is the inflaton potential. This yields the comoving curvature perturbation

$$\begin{aligned}\zeta &= \frac{2}{3}\frac{\mathcal{H}^{-1}\partial\Phi/\partial\tau + \Phi}{1+w} + \Phi \\ &= \frac{-M\alpha_1 V'}{3}\left(\frac{\tilde{x}}{1+w} + \tau + \tilde{x}\right)\Theta(\tau + \tilde{x}) \approx \lambda\tilde{x}\Theta(\tilde{x}),\end{aligned} \quad (4)$$

where $w \simeq -1$ during inflation and $\lambda \equiv -\alpha_1 M V'(2 + w)/(3 + 3w) \sim \alpha_1 M V/V'$ sets the late-time amplitude. The final, approximate equality, is valid late in the inflationary epoch.

Results: Using superhorizon curvature perturbations ζ_i at inflation-end and a set of *linear transfer functions* $\tilde{\Delta}_X$ the perturbed distribution of observable X at later times is

$$\Delta_X(\mathbf{x},\hat{n},\tau) = \int d^3k\, e^{i\mathbf{k}\cdot\mathbf{x}}\tilde{\Delta}_X(k = |\mathbf{k}|,\hat{n},\tau)\zeta_i(\mathbf{k})\,, \quad (5)$$

where $\Delta_X(\mathbf{x},\hat{n},\tau)$ is the local value of observable X (e.g., $\delta T/T$) at position $\mathbf{x}$, time τ, in sky direction $\hat{n}$, and $\mathbf{k}$ is a comoving wave-vector. Moments of $\Delta_X(\mathbf{x},\hat{n},\tau)$ are, e.g., density or velocity as a function of $\mathbf{x}$, while $\Delta_X(0,\hat{n},\tau)$ is the anisotropy at Earth. We compute the transfer functions, which encode the evolution of the coupled multi-component fluid/gravity system, using a customized CAMB [12] code in a WMAP 7-year best-fit cosmology [13], and our own code to find 3D Fourier transforms precise enough to determine accurate observables.

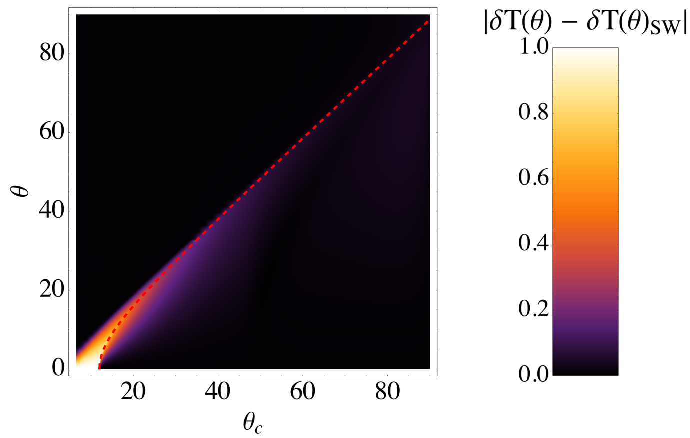

FIG. 1. The difference between the actual angular profile of $\delta T/T$ as a function of θ_c and the Sachs-Wolfe truncated-dipole approximation. The dashed line shows the maximum extent of the disc in the Sachs-Wolfe approximation. Acoustic spreading extends the radius and alters the detailed shape of small discs.

Temperature: In the Sachs-Wolfe (SW) limit [14], CMB temperature anisotropies are just $\delta T(\theta,\phi)/T \propto \zeta(\vec{x},\tau_{dc})$, where $|\vec{x}| = D_{dc}$ is the distance to last scattering and coordinates can be chosen so that $x = D_{dc}\cos\theta$. In this limit the wake gives rise to a simple perturbation $\delta T/T \propto \Theta(\theta_c^{\rm sw}-\theta)\,(\cos\theta - \cos\theta_c^{\rm sw})$, where $\theta_c^{\rm sw} = \cos^{-1} x_c/D_{dc}$ is the angular radius of the disc in the SW limit [8, 10]. Yet, ζ is constant only on super-horizon scales and non-SW effects contribute to $\delta T/T$. We evolve the cosmic wake solution between reheating and decoupling to find the actual $\delta T/T$ profile. These results are shown in Fig. 1 as the difference between the actual cosmic wake solution and the SW approximation. A range of x_c is shown with one axis the angular edge of the profile $\theta_c \equiv \cos^{-1}[(x_c - r_{sh})/D_{dc}]$, where r_{sh} is the sound horizon at decoupling, and the other the angle θ from center. We find $|\delta T/T|$ is largest at profile center, decreases nearly-linearly in $\cos\theta$, and smoothly transitions to a constant at $\theta = \theta_c$ with no edge or discontinuity. The width of the transition region is roughly the angular separation between the two polarization peaks discussed below.

Polarization: CMB photons are linearly polarized by Thomson scattering off free electrons [15, 16]. This occurs both near decoupling ($z_{dc} \sim 1100$) and after reionization ($z_{re} \sim 10$). Net polarization proportional to the quadrupole of the radiation incident on the electrons is created. Scattering at decoupling depends on known atomic physics [17], but the exact reionization history of the Universe is unknown. As our key results are not very sensitive to the reionization history we choose a simple fiducial reionization model consistent with [13].

Linear polarization of an electromagnetic wave is characterized by Stokes parameters Q and U. In coordinates with a wake profile centered at $\theta = 0$ polarization is purely E-mode and $U = 0$. The polarization pattern is radial (azimuthal) for a cold (hot) disc with $Q > (<)\, 0$.

We parametrize polarization from a single wake by $Q(\theta)$, and find qualitative differences for small ($\theta_c \lesssim 12°$) and large discs. In Fig. 2 we show the cases $\theta_c \approx 10°$ and $\theta_c \approx 60°$. Large discs have a distinct "double peak"; two rings of sharply enhanced polarization concentric with the affected temperature disc. This is a characteristic of cosmic wakes and occurs provided $\theta_c \gtrsim 12°$. Fig. 3 shows the polarization pattern for wakes with $5° < \theta_c < 90°$.

Why a double peak?: The double peak is a striking feature, but the physics that gives rise to it is simple. At the end of inflation, the perturbation in the Newtonian potential is $\Phi \sim \tilde{x}\,\Theta(\tilde{x})$. Between inflation-end and decoupling, a linear-in-x perturbation (like $\Phi = C\tilde{x}$) remains so as the Φ equations are second order in spatial derivatives. By contrast, the kink at x_c spreads at the sound-speed $c_s \lesssim c/\sqrt{3}$ of the plasma into a smooth profile confined to the sound horizon of x_c until matter-radiation (MR) equality when $c_s \to 0$. Yet, at the sound horizon at any time, the first derivative remains almost discontinuous. An electron near an edge of this region polarizes a relatively large fraction of light as the quadrupole moment is sensitive to the second derivative of the perturbation. The two edges of the region at decoupling are separated by twice the sound horizon $2r_{sh} \sim 306$ Mpc or $r_{sh}/D_{dc} \approx 1/90$ [13]. The angle between edges is $\theta_s \approx \cos^{-1}[(x_c - r_{sh})/D_{dc}] - \cos^{-1}[(x_c + r_{sh})/D_{dc}]$, which is borne out in our numerical solution. For $\theta_c \approx 90°$ this width is $\theta_s \approx 2\theta_{sh} = 1.3°$. For smaller discs, θ_s is larger, and for $\theta_c \lesssim 12°$ the inner peak disappears entirely.

Density: After MR equality, c_s is small and the edge of the cosmic wake is frozen. Due to perturbation growth the amplitude of the density perturbation at the edge of the wake today is larger by a factor $z_{dc} \sim 1100$ relative to decoupling. As a Newtonian potential $\Phi = C\tilde{x}\theta(\tilde{x})$ includes a δ-function density perturbation at x_c, a planar sheet of over/under-density (for hot/cold discs in the CMB, respectively) centered at $x \approx D_{dc}\cos\theta_c$ is expected with a thickness set by r_{sh} at equality. This is confirmed numerically in Fig. 4, where we show the dark matter density contrast in conformal Newtonian gauge (baryons look similar). Such a mass sheet could lead to signatures in LSS or lensing surveys which, combined with CMB data, could further corroborate a cosmic wake detection. We leave this investigation to future work.

Detectability: We now estimate detectability of the polarization signal for varying θ_c and intensity by several current and future experiments. CMB signals of a wake are circularly symmetric and we orient coordinates with disc-center at $\theta = 0$; a rotation would center it elsewhere.

To estimate a detection threshold we fit to a one parameter model for the amplitude A of temperature at disc-center. We consider temperature (T) alone, E-mode polarization (E) alone, and E combined with information from the T map and cross-correlation. We work in l-space where the noise covariance is diagonal. Circular

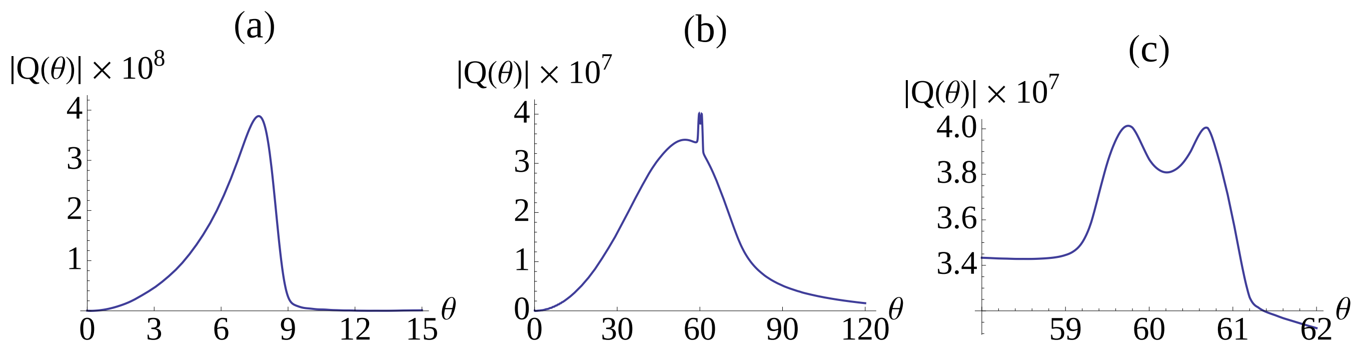

FIG. 2. Polarization for (a): $\theta_c \approx 10°$; (b): $\theta_c \approx 60°$, with $|\delta T/T| = 10^{-4}$ at center. The double peak in (b) is magnified in (c).

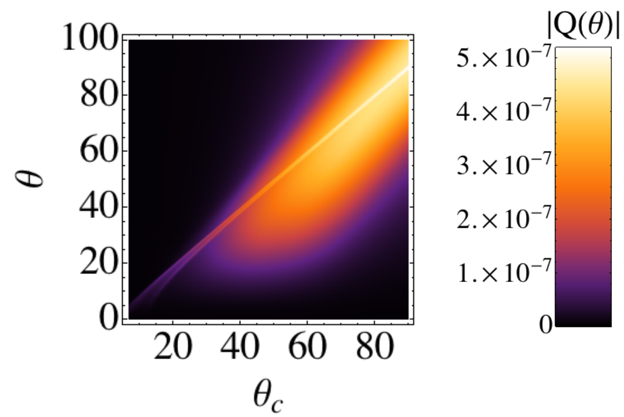

FIG. 3. Density plot of $|Q(\theta)|$ as a function of θ_c.

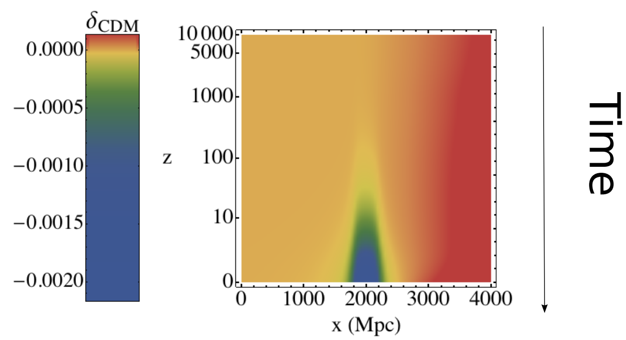

FIG. 4. $\delta_{\rm cdm}$ evolution. This wake has $\theta_c \approx 80°$ and $\delta T/T = -10^{-4}$ at CMB disc center.

symmetry allows the azimuthal angle φ to be integrated out (so in l-space $a^{T,E}_{l,m}$ do not contribute if $m \neq 0$).

We include CMB fluctuations in T and E consistent with WMAP-7 concordance parameters [13] as well as noise realizations for each detector up to $l_{max} = 2000$. We add a wake to this and compute the relative likelihood function (which amounts to a simple χ^2 in this one parameter model) to determine if it is detectable. We normalize so that for a given disc a no detection is consistent with $A = 0$ (only Gaussian fluctuations) and a good detection has $A = 1$. We project sensitivities for

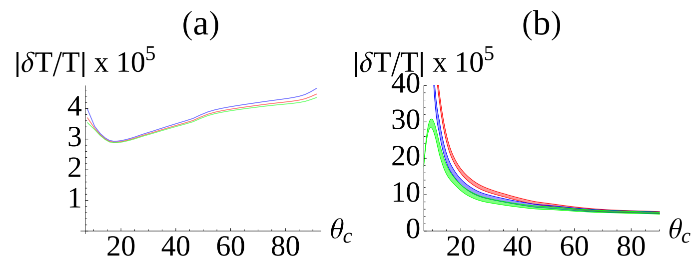

FIG. 5. 3σ detectability threshold for (a) T and (b) E-mode polarization for Planck (Red), SPIDER (Blue), and CMBPol (Green). In (b) line-thickness indicates the the extent to which cross-correlation is used to enhance the measurement.

three experiments: the Planck satellite mission [18], a balloon mission like SPIDER [19] and a satellite mission like CMBPol (EPIC-2m) [20]. We use the same sensitivities, beam-widths, weight per solid angle, and observing time as [21] (we assume sensitivity to Stokes I is $\sqrt{2}$ that of Q and U). We analyze these three, but any experiment that measures the T or E over a significant fraction of the sky has the potential to detect a cosmic wake.

As we fit for a_{lm} rather than power spectra C_l, a cut sky induces straightforward but bothersome complications (spherical harmonics are no longer orthonormal). To get simple estimates we use a full sky instead. For all-sky missions this amounts to ignoring foreground effects, while for partial sky-coverage missions we further assume Gaussian fluctuations are statistically similar across the sky. A full treatment of these effects would likely decrease quoted sensitivities by a modest factor.

We do a combined analysis across all bands. For each θ_c and experiment we find the minimum $|\delta T/T|$ at profile center such that a detection of $A = 1$ is 3σ away from zero. This represents a conservative estimate of the detection threshold in T and E. We summarize our findings in Fig. 5. For E we can also use information from TE cross-correlation, which increases sensitivity by allowing the expected E signal correlated with T to be subtracted from Gaussian fluctuations. A sensativity band ranging from full TE correlation to none is shown in Fig. 5(b).

For small discs ($\theta_c \lesssim 10°$), $|\delta T/T| > 4 \times 10^{-5}$ is likely observable in T, but must be brighter than $\sim 2 \times 10^{-4}$

to be observable in E. A search for cosmic wakes in the T map was recently carried out [22, 23] using WMAP-7 data. While the analysis found several anomalous features, it rules out wakes with $|\delta T/T| > 10^{-4}$. Thus, while the potential exists to observe small discs in the T map, correlating them with E signals is likely only possible at below the 3σ level, evidence not likely significant enough to exclude other potential explanations. For $\theta_c \gtrsim 25^\circ$ the situation is much more promising. Fainter discs are detectable in E, and very large discs are detectable almost as easily in E as T. This is clear from Fig. 3. Large discs have a coherent E signal over a larger angular range and can be found more easily over Gaussian fluctuations and noise. Further, for $\theta_c > 12^\circ$ they have a distinctive double peak feature on small scales. This angular size dependence is particularly important because the size distribution of collision discs, $dN(\theta_c) \propto \sin\theta_c d\theta_c$, is a robust prediction of the theory [9]. The analysis of [22, 23] was for $\theta_c \lesssim 11^\circ$, which with this distribution are much less common than larger discs.

Conclusions: We have found the real-space evolution of the cosmic wakes produced by collisions between bubble universes, and determined the distinctive temperature and polarization patterns they imprint on the CMB. These patterns have circular symmetry reflecting the near-planar symmetry of cosmic wakes, and the polarization pattern can have a distinct double-peak structure due to propagation of acoustic waves in the primordial plasma. We estimated the detectability of cosmic wakes by planned CMB experiments in both temperature and polarization. Holding fixed $\delta T/T$ at disc center and varying the angular size θ_c, larger discs get *easier* to detect with polarization, but harder to detect with temperature (Fig. 5). Detection of a cosmic wake would show our observable Universe is part of a larger multiverse, support the idea of a string theory landscape, and be an astounding revelation of the nature of the big bang.

Acknowledgements: We thank G. D'Amico, S. Chang, B. Freivogel, R. Gobbetti, G. Hinshaw, L. Hui, E. Lim, A. Moss, J. Roberts, I. Sawicki, R. Scoccimarro, I-S. Yang, M. Zaldarriaga, and J. Zibin for discussion. KS thanks PI and the ACP, where some of this work was done. MK is supported by NSF CAREER grant PHY-0645435. KS is supported by a NSERC of Canada Discovery grant. TSL is supported by NSERC and an IPP Theory Fellowship.

[1] M. Kleban arXiv:1107.2593 [astro-ph.CO].
[2] A. Aguirre and M. C. Johnson, Rept. Prog. Phys. **74**, 074901 (2011).
[3] S. W. Hawking *et al.*, Phys. Rev. **D26**, 2681 (1982).
[4] J. Garriga *et al.*, Phys. Rev. **D76**, 123512 (2007).
[5] B. Freivogel *et al.*, JHEP **05**, 090 (2007).
[6] S. Chang *et al.*, JCAP **0804**, 034 (2008).
[7] R. Gobbetti and M. Kleban(2012), arXiv:1201.6380 [hep-th].
[8] S. Chang *et al.*, JCAP **0904**, 025 (2009).
[9] B. Freivogel *et al.*, JCAP **0908**, 036 (2009).
[10] B. Czech *et al.*, JCAP **1012**, 023 (2010).
[11] V. F. Mukhanov *et al.*, Phys. Rept. **215**, 203 (1992).
[12] A. Lewis *et al.*, Astrophys. J. **538**, 473 (2000).
[13] E. Komatsu *et al.* arXiv:1001.4538 [astro-ph.CO].
[14] R. Sachs and A. Wolfe, Astrophys. J. **147**, 73 (1967).
[15] J. Bond and G. Efstathiou, Astrophys. J. **285**, L45 (1984).
[16] M. Zaldarriaga and U. Seljak, Phys. Rev. **D55**, 1830 (1997).
[17] S. Seager *et al.*, Astrophys. J. **523**, L1 (1999).
[18] Planck(2006), arXiv:astro-ph/0604069.
[19] B. P. Crill *et al.* arXiv:0807.1548 [astro-ph].
[20] D. Baumann *et al.*, AIP Conf. Proc. **1141**, 10 (2009).
[21] Y.-Z. Ma *et al.*, JCAP **1010**, 007 (2010).
[22] S. M. Feeney *et al.*, Phys. Rev. Lett. **107**, 071301 (2011).
[23] S. M. Feeney *et al.*, Phys. Rev. **D84**, 043507 (2011).